Article

Discovery Medicine 2024; 36(185): 1306–1315
https://doi.org/10.24976/Discov.Med.202436185.121

Proteomic Analysis of Butyrate-Resistant Colorectal Cancer-Derived Exosomes Reveals Potential Resistance to Anti-Cancer Drugs

Kesara Nittayaboon[1], Kittinun Leetanaporn[1], Surasak Sangkhathat[1], Sittiruk Roytrakul[2], Raphatphorn Navakanitworakul[1,*]

[1]Department of Biomedical Sciences and Biomedical Engineering, Faculty of Medicine, Prince of Songkla University, 90110 Hat Yai, Songkhla, Thailand
[2]Functional Ingredients and Food Innovation Research Group, National Center for Genetic Engineering and Biotechnology (BIOTEC), National Science and Technology Development Agency, 12120 Khlong Luang, Pathumthani, Thailand
*Correspondence: nraphatp@medicine.psu.ac.th (Raphatphorn Navakanitworakul)
Published: 20 June 2024

Background: Butyrate-resistant (BR) cells play an important role in acquiring chemoresistance in colorectal cancer (CRC). Our previous study demonstrated that BR CRC cells showed cross-resistance to chemotherapy drugs, including 5-fluorouracil and oxaliplatin, in both monolayer and spheroid cultures. The mechanisms underlying drug resistance were also elucidated. However, the link between parental (PT) and BR cells remains unclear. Extracellular vesicles (EVs) are key cell-cell communications that transport various molecules, including DNA, RNA, and proteins, between the donor and target cells. EVs contribute to drug resistance in cancers, such as melanoma and lung cancer. Recently, we focused on the correlation of proteomic profiles of EVs from different cell types.

Methods: In this study, we analyzed the proteomic profiles of EVs derived from PT and BR cells to investigate the mechanisms underlying the butyrate- and chemo-resistant phenotypes. EVs were isolated from PT and BR cells using ultracentrifugation. The characteristics of the EVs were evaluated using western blot and transmission electron microscopy. The EV proteomic data were further analyzed using liquid chromatography-mass spectrometry.

Results: We identified a unique protein expressed in BR cells related to the chemoresistant phenotype. Functional enrichment analysis showed that BR cells had higher protein catalytic activity, binding, and transcription activity. The STITCH database showed a greater correlation between protein-drug interactions in BR cells than in PT cells. Moreover, our findings support the hypothesis that EVs promote tumor progression and metastasis and affect the tumor microenvironment.

Conclusions: Proteomic analysis of EVs from BR CRC cells reveals insights into drug resistance mechanisms, including protein-mediated carcinogenesis and reduced drug uptake, offering potential strategies to overcome resistance in clinical practice.

Keywords: BR cells; chemoresistance; EVs; drug resistant mechanism; proteomics

Introduction

Colorectal cancer (CRC) is an urgent public health issue, including in Thailand, with high rates of morbidity and mortality. CRC treatments such as surgery and chemotherapy are effective. However, approximately 40–50% of patients who receive only curative surgery and 20–30% who receive adjuvant chemotherapy subsequently relapse, develop metastatic disease, and die. Multidrug resistance in cancer is the main reason for this relapse, leading to anticancer drug resistance, treatment failure, and poor survival outcomes [1]. The 5-fluorouracil (5-FU) overall monotherapy response rate in advanced CRC patients is limited to 10–15% [2]. A previous study revealed that an increase in butyrate-producing bacteria in patients with CRC correlated with poor prognosis and poor response to treatment [3]. Moreover, a connection between butyrate resistance and chemoresistance has been proposed. Previous studies on CRC cell lines have shown that butyrate-resistant (BR) cells also resist chemotherapy drugs, including 5-FU, doxorubicin, oxaliplatin (Oxa), and tricostatin [4–6]. Moreover, these cells exhibit aggressive behaviors, including migration and invasion. However, the relationship between butyrate resistance and chemoresistance has not been elucidated. Although, it has been hypothesized that cells communicate and transfer proteins, nucleic acids, or lipids from resistant donor cells to the target cells.

Extracellular vesicles (EVs) are nano-sized vesicles derived from cells that mediate cell-to-cell communication by transporting bioactive molecules. EVs play an important role in various physiological and pathological conditions. EVs in cancer can transport specific cargo, especially pro-

teins and RNAs, that affect drug efflux and regulate the signaling pathways involved in epithelial-mesenchymal transition, autophagy, metabolism, and cancer stemness [7,8]. The proteomic content of EVs or proteomic EV cargo reflects the pathological status of patients and may be used for diagnosis, prognosis, and prediction [8,9]. Several bioinformatic tools and databases have been used to determine differences between patient groups [10–12].

In the present study, we aimed to elucidate the link between butyrate- and chemo-resistant phenotypes using proteomics. The proteomic patterns between parental (PT) and BR EVs were characterized and compared. Our findings revealed that EVs from BR cells focus on enzymes with catalytic and modified activities, whereas EVs from PT cells focus on metabolic maintenance. Moreover, interactions between proteins in BR-derived EVs and drugs may be associated with drug resistance during cancer treatment. These findings contribute to a better understanding of EVs in CRC cell biology and provide a basis for further research on candidate predictive biomarkers.

Materials and Methods

Cell Culture and EV Isolation

Human epithelial colorectal carcinoma cells HCT-116 (ATCC; CCL-247, University Boulevard, Manassas, VA, USA) and PMF-Ko14 (Riken: RBC1426, Koyadai, Tsukuba, Ibaraki, Japan) were cultured in Dulbecco's Modified Eagle Medium (2556764, Gibco™ Thermo Fisher Scientific, Waltham, MA, USA) supplemented with 10% fetal bovine serum with 56 °C heat-inactivated (FBS; 42G9391K, Gibco™ Thermo Fisher Scientific, Waltham, MA, USA) combined with 1% penicillin/streptomycin (171334, Gibco™ Thermo Fisher Scientific, Waltham, MA, USA) in a humidified incubator with an atmosphere of 5% CO_2 at 37 °C. BR CRC cells were established and characterized previously [5,6] and grown under the same conditions as their PT cells. This project is exempt from the Research Ethics Committee (REC) Faculty of Medicine, Prince of Songkla University's review process under reference number REC6337942. For the mycoplasma detection, we maintained the cell, routinely checked the cell morphology, and tested the butyrate sensitivity to confirm the characteristics of cells in accordance with previous research [5,6]. For EV isolation, cells were seeded at 80% confluence in a 10-cm cell culture dish and maintained in Dulbecco's Modified Eagle Medium supplemented with 10% heat-inactivated and EV-deplete FBS medium. The BR and PT cells were collected after 24 h of incubation. FBS with EV depletion was used as an EV collection medium. The EV-deplete FBS was prepared by ultracentrifugation at 110,000 ×g for 16 h at 4 °C, and the supernatant was utilized. Media were collected and differential centrifugation was performed. Initially, the media were centrifuged to eliminate cell debris and apoptotic bodies at 2500 ×g for 30 min at 4 °C. The supernatant was then centrifuged at 20,000 ×g for 60 min at 4 °C, and the final supernatant was ultracentrifuged at 110,000 ×g for 2 h, at 4 °C to pellet the EVs (CTZ17H15, Beckman Coulter, Brea, CA, USA).

EVs Characterization

After the differential centrifugation step, pellets were resuspended in phosphate-buffered saline. Western blot and electron microscopy were performed using a JEM-2101 transmission electron microscope (TEM; Talos F200i, Thermo Fisher Scientific, Waltham, MA, USA) to confirm the presence of EVs in isolates. The electron microscopy examination protocol has been previously described [13]. The EV samples were fixed in 2.5% glutaraldehyde and then loaded onto grids coated with carbon copper. The grids were then cleaned with Dulbecco's phosphate-buffered saline (14190144, Thermo Fisher Scientific, Waltham, MA, USA) and distilled water. Before examination, 1% uranyl acetate was used to stain the grid. For western blot, standard SDS-PAGE and immunoblotting were performed using EV-positive markers, including CD9 (cat. no. 13174; Cell Signaling Technology, Inc., Danvers, MA, USA), CD81 (cat. no. SC-166029; Santa Cruz Biotechnology, Dallas, TX, USA), and CD63 (cat. no. 55051; Cell Signaling Technology, Inc., Danvers, MA, USA) as well as Alix (cat. no. 2171; Cell Signaling Technology, Inc., Danvers, MA, USA) for identifying the presence of EVs. Cytochrome C (cat. no. 4272T; Cell Signaling Technology, Inc., Danvers, MA, USA) negativity confirmed the absence of co-isolated contaminating cell debris [14]. The primary antibody at dilution 1:500 was incubated overnight, whereas the compatible secondary antibody at dilution 1:1000 was incubated for 2 hrs.

Proteomic Analysis

All EV samples were subjected to mass spectrometry at the Functional Proteomics Technology Laboratory, National Center for Genetic Engineering and Biotechnology (BIOTEC), Thailand. EV pellets from PT and BR cells were processed as described previously [5,6] and analyzed by liquid chromatography-mass spectrometry (UltiMate 3000 Nano/Capillary, Bruker Life Science Mass Spectrometry, Impact II, San Jose, CA, USA). The DeCyder MS differential analysis program (version 2.0; GE Healthcare, Chicago, IL, USA) was used to quantify and identify differentially expressed proteins, and the MASCOT search engine (version 2.8.3, Matrix Science, London, UK) was based on the NCBI human protein databases. Proteins differentially expressed among EVs from each cell type were analyzed for pathway enrichment by Kyoto Encyclopedia of Genes and Genomes (KEGG) analysis by R-studio (version 4.1.1; R Foundation for Statistical Computing, Vienna, Austria). PANTHER (version 16.0, https://pantherdb.org/) and UniProt software (https://www.uniprot.org/) were utilized to classify proteins expressed uniquely in every cell type.

Data Analysis

After collecting the proteins, the free functional enrichment analysis tool FunRich (http://www.funrich.org/) generated a Venn diagram. Data from the VesiclePedia database were retrieved using the FunRich plugin for EVs, and the ExoCarta exosome database (http://www.exocarta.org/) was utilized. The PANTHER database (version 16.0, https://pantherdb.org/) analyzed unique proteins from the Venn diagram for their molecular functions, biological processes, and protein classes. The unique protein datasets were then analyzed for protein-protein interactions using the STRING database (Version 12.0, https://string-db.org/) and for protein-drug interactions using the STITCH database (Version 5.0, http://stitch.embl.de/).

Statistical Analysis

The statistical analysis analyses used GraphPad Prism Software (version 9.00 for macOS; GraphPad, San Diego, CA, USA). The Student's *t*-test (two-tailed) was used to compare two independent group means, while one-way or two-way ANOVA (followed by Tukey or Sidak's multiple comparison tests) compared more than two independent group means. p values < 0.05 were considered statistically significant.

Results

Quantification of EVs

Cellular morphology of PT and BR cells was captured by an inverted light microscope (IX71, Olympus, Hachioji-shi, Tokyo, Japan). There is a slight difference between PT and BR cells as shown in Fig. 1A. The BR cells showed an increase of vacoularization and cellular volume, represented in black and white arrows respectively. TEM and western blot analyses characterized the presence of EVs. Fig. 1B showed the EV morphology at 11,000× magnification. The TEM results showed a circular cup shaped vesicle with a diameter of approximately 100–200 nm, indicated by the black arrow. Western blot analysis, shown in Fig. 1C and **Supplementary Fig. 1**, demonstrated a positive signal for the EV-positive markers CD9, CD81, CD63, and Alix in isolated EV samples. The negative marker, cytochrome C, showed a no signal in the EV sample and a positive signal in the cell lysate.

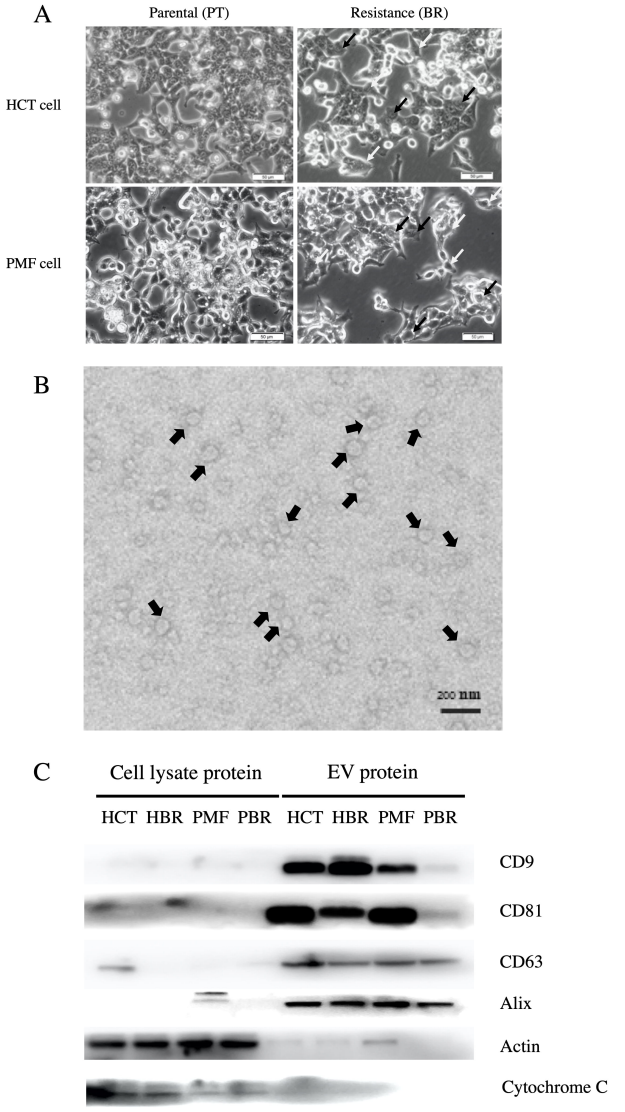

Fig. 1. The quantities of extracellular vesicles (EVs) and their characterization. (A) Cellular morphology of HCT-116 and PMF-ko14 and their butyrate-resistant (BR) cells. The increasing of vacoularization (black arrow) and cellular volume (white arrow) are indicated in the picture. Scale bar = 50 µm. (B) Image of EVs from transmission electron microscopy. The bold black arrows indicated EVs. Scale bar = 200 nm. (C) Western blot analysis showed the presence of EVs through the EV-positive markers CD9, CD63, and CD81, and the absence of co-isolated contaminants of cell debris through the EV-negative marker, Cytochrome C. PT, parental.

EV Proteome Profiling by Mass Spectrometry

Principal component analysis (PCA) of the proteomic data was performed to investigate the differences in protein expression. The data were plotted in a 2-dimensional graph of PC1 and PC2 showing values of 16.23% and 13.91%, respectively (Fig. 2A). The Venn diagram identified shared and uniquely expressed proteins in each cell type. The left panels of Fig. 2B,C represented the protein comparison between EVs from PT and BR in HCT and PMF cell lines. Shared proteins represented the main characteristics of CRC cell lines, while unique proteins may be associated with the BR status. Interestingly, the unique protein content of the BR-derived EVs was higher than that of the PT-derived EVs in both cell types.

Furthermore, the right panels of Fig. 2B,C displayed a Venn diagram from the EV database, highlighting unique proteins in each cell type. We input data from two EV

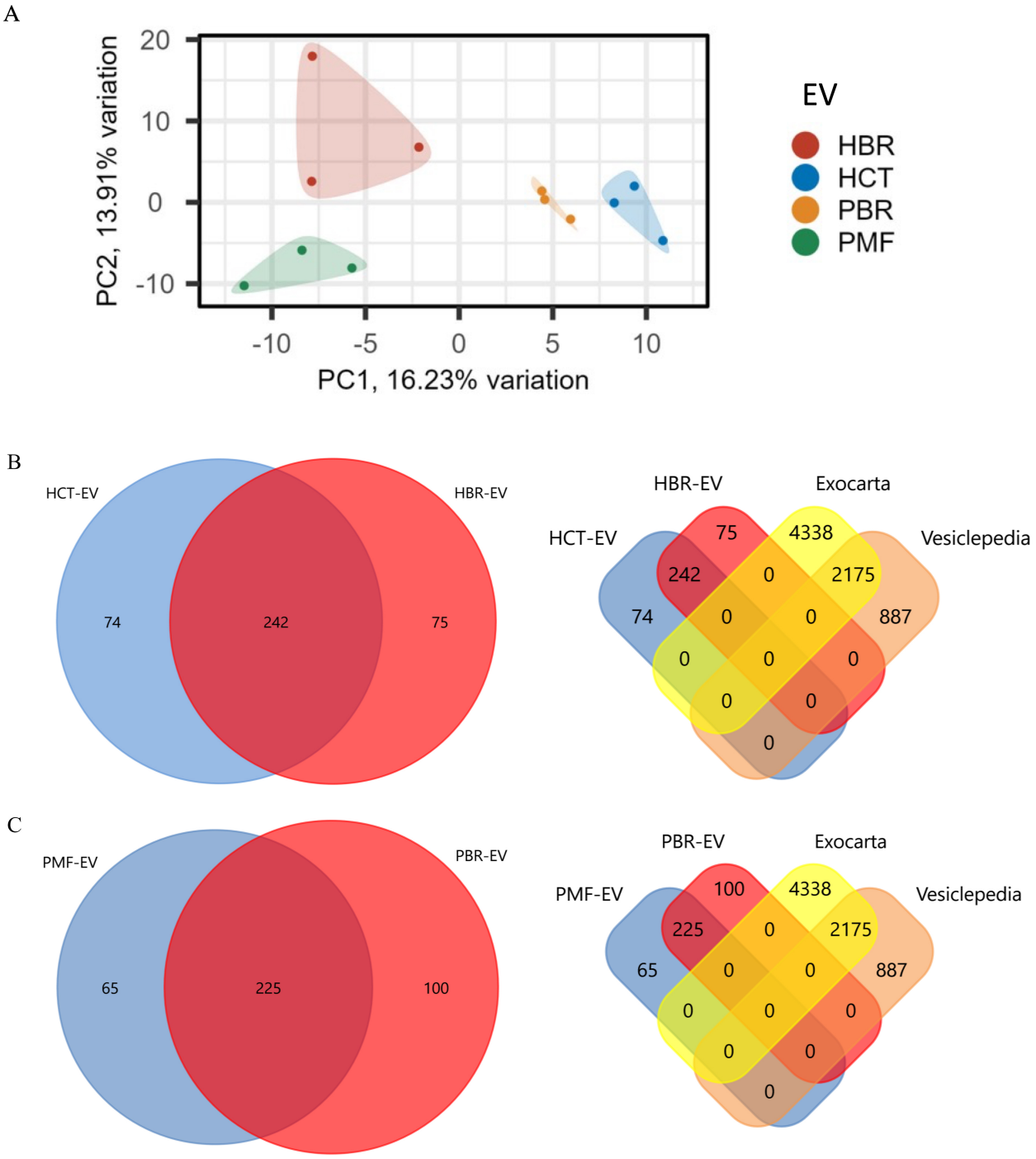

Fig. 2. Mass Spectrometry-based profiling of EV proteome. EV from HCT and PMF BR and non-resistant PT cancer cell lines were analyzed by mass Spectrometry. (A) Principal component analysis (PCA) plot of difference in protein expression. (Left panel of B and C) Venn diagram showing shared and unique proteins expressed in HCT-, HBR-, PMF-, and PBR-derived EVs. (Right panel of B and C) Venn diagram showing proteins from isolated EVs and two EV databases: VesiclePedia and ExoCarta.

databases: VesiclePedia and ExoCarta. Based on these results, we found the proteins not included in the database for any cell type.

BR-Derived EVs Exert Catalytic Activity, Transcription Regulator Activity, and Biological Regulation

Functional enrichment analysis using results from the PANTHER database analysis of unique proteins in each EV-derived cell type is shown in Fig. 3. Fig. 3A pre-

sented a bar graph depicting a higher number of resistant EV proteins involved in molecular functions such as binding, as well as molecular transducer, catalytic, and transporter activities. The high expression of these proteins may be correlated with the adaptation of cells to survive in the presence of butyrate during the butyrate-induction step. The results from the biological processes shown in Fig. 3B also indicated an abundance of proteins involved in metabolic processes, responses to stimuli, biological regulation, localization, and cellular processes, especially in PBR-EVs. Moreover, Fig. 3C highlighted the abundance of resistant EV protein classes including metabolite interconversion enzymes, gene-specific transcriptional regulators, transmembrane signal receptors, cell adhesion molecules, transporters, and protein-modifying enzymes.

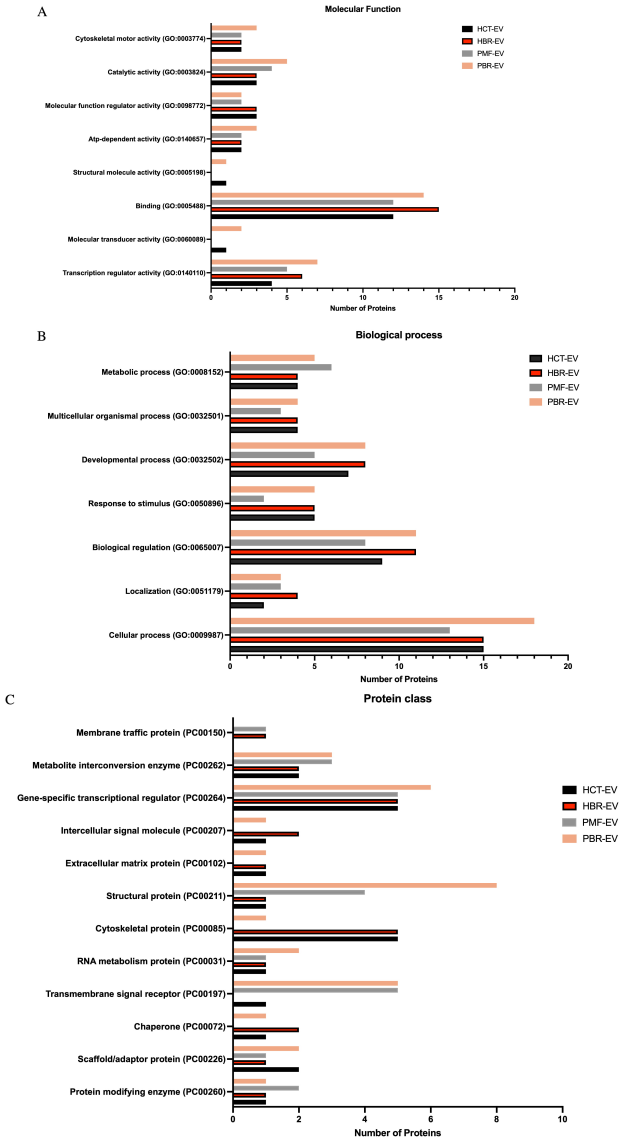

Fig. 3. Functional enrichment analysis of the unique proteins. (A) Molecular function. (B) Biological process. (C) Protein class. GO, Gene ontology.

The STRING database was used to examine the protein-protein interactions of distinct proteins from EVs in each cell type. Fig. 4 showed the protein network of EVs in each cell type. Fig. 4A,B represented the STRING correlation of HCT-EVs and HBR-EVs, respectively. While Fig. 4C,D represented PMF-EVs and PBR-EVs, respectively. Fig. 4E showed the status of the network. Tables 1,2 showed the molecular functions and KEGG pathways analyzed using the STRING database. In the context of multiple testing within each category, the false discovery rate (FDR) referred to *p* values adjusted using the Benjamini-Hochberg procedure for accounting for the inflation of significance levels. Interestingly, the molecular functions enriched in PBR-EVs were proteasome-related proteins, while their parental PMF-EVs were enriched with heat shock-related proteins. The KEGG pathways showed high enrichment of proteins in the ribosomes of HCT-, HBR-, and PMF-EVs, whereas PBR-EVs showed proteasome pathway enrichment. The proteasome plays a crucial role in regulating the level and function of proteins involved in cancer cell proliferation, inhibition of chemotherapy-induced apoptosis, and the developing drug resistance. Proteasome inhibition has been postulated as a new target for anti-cancer drugs.

We further determined protein-drug interactions using the STITCH database. Fig. 5 showed the protein-drug interactions of unique EV proteins in each cell type and drug (5-FU and Oxa). We added the 5-FU-correlated protein, single-strand-selective monofunctional uracil-DNA glycosylase 1 (SMUG1), which removes uracil, 5-formyluracil, and uracil derivatives from ssDNA and dsDNA. We correlated them with biomarkers of aggressive phenotype, DNA repair, cell cycle, and apoptosis [15]. We also added Oxa-related proteins, including solute carrier family 47 member 1 (SLC47A1), a multidrug efflux pump, and solute carrier family 22 member 2 (SLC22A2), an organic cation transporter. Previous research demonstrated that HCT-BR cells resist Oxa and PMF-BR cells resist to 5-FU [6].

Fig. 5A,B showed the interaction of the drugs and unique proteins in HCT- and HBR-EVs, respectively. The red rectangle indicated drug input. Fig. 5C,D represented the interaction between the drugs and unique proteins in PMF-EVs and PBR-EVs, respectively. Interestingly, the drug-protein interaction in PT EVs showed a lower number of nodes and edges than that in resistant EVs, as shown in Fig. 5E. The functional enrichment of the network was analyzed. The KEGG pathway from the PT EV was ribosome, while more pathways were shown in the resistant EV, including the Proteasome, and RNA polymerase. Table 3 shows an enrichment analysis of the KEGG pathway from the STITCH database.

Differentially expressed proteins are shown in the volcano plot. Fig. 6A represented proteins compared between HCT-EVs and HBR-EVs, while Fig. 6B identified the proteins between PMF-EVs and PBR-EVs. Green dots repre-

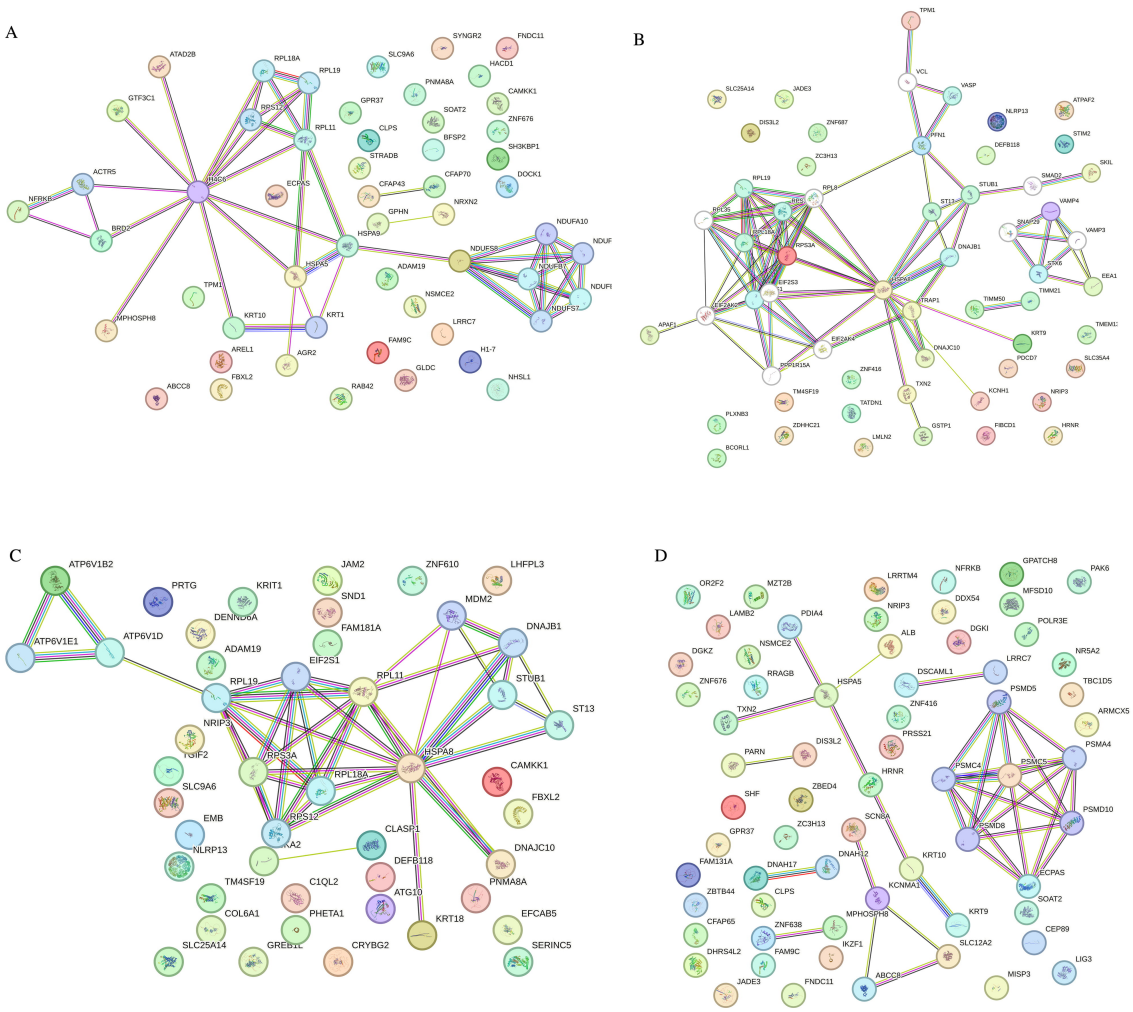

E

Network Stats	HCT-EV	HBR-EV	PMF-EV	PBR-EV
number of nodes:	53	57	46	64
number of edges:	46	84	40	34
average node degree:	1.74	2.95	1.74	1.06
avg. local clustering coefficient:	0.394	0.456	0.332	0.344
expected number of edges:	35	59	26	23
PPI enrichment p-value:	0.0494	0.00106	0.0079	0.0149

Fig. 4. Protein-protein interaction network of unique proteins in each cell type from the STRING database. The protein interaction of EVs from HCT (A), HBR (B), PMF (C), and PBR (D) are illustrated. The network status of each EV cell is shown in (E).

sented non-significant expression in both cell types, while red dots represented significant up- or down-regulation. We found that the levels of proteasome pathway (DLGAP5), cytoskeleton (CEP170 and LAMB2), ribosomal (RPL11), and cell regulation (FASTK, GLS2, and FOCAD) proteins were higher in HBR-derived EVs than in their parental HCT-derived counterparts. Meanwhile, the protein levels of transcriptional regulators (ZBTB11, DEPDC1, KDM3B, WARS, and TP53), as well as receptor (GRM5, RRAGB, and GPR143) and transporter (COPB1) proteins were decreased.

For the PMF cells, we found upregulation of proteins involved in signal transduction (ZDHHC21, SH3KPB1, ZBED4, HSP90AA1, and ZNF687), cytoskeleton proteins (DNAH2 and PRTG), ribosomal proteins (RPS3A and RPSA), and the proteasome (NPEPPS). In contrast, the proteins involved in cell apoptosis and proliferation (ANGPT2, TXN2, and STRADB), signal transduction (PLD1, ITPR3, and ZNF567), and transcriptional regulation (WARS) were decreased. The top 15 proteins with up and downregulation in HCT and PMF cell types are listed in Tables 4,5, respectively. The list of total proteins were shown in **Supplementary Tables 1,2**.

Table 1. Molecular function (Gene ontology) from STRING analysis.

Cell type	GO-term	Description	Count in network	Strength	FDR
HCT-EV	GO:0008137	NADH dehydrogenase (ubiquinone) activity	6 of 41	1.74	1.4×10^{-5}
	GO:0009055	Electron transfer activity	7 of 121	1.33	4.0×10^{-5}
	GO:0015399	Primary active transmembrane transporter activity	7 of 170	1.18	2.5×10^{-4}
	GO:0022804	Active transmembrane transporter activity	8 of 421	0.85	8.6×10^{-3}
HBR-EV	GO:0030544	Hsp70 protein binding	4 of 47	1.47	2.7×10^{-2}
	GO:0031072	Heat shock protein binding	6 of 126	1.22	1.1×10^{-2}
	GO:0003735	Structural constituent of ribosome	6 of 169	1.09	2.7×10^{-2}
	GO:0003723	RNA binding	16 of 1672	0.52	2.7×10^{-2}
PMF-EV	GO:0030544	Hsp70 protein binding	4 of 47	1.56	2.9×10^{-2}
	GO:0031072	Heat shock protein binding	5 of 126	1.23	3.2×10^{-2}
PBR-EV	GO:1902494	Catalytic complex	16 of 1539	0.51	1.1×10^{-2}
	GO:0140535	Intracellular protein-containing complex	11 of 784	0.64	1.5×10^{-2}
	GO:0022624	Proteasome accessory complex	4 of 24	1.71	9.9×10^{-4}
	GO:0005838	Proteasome regulatory particle	3 of 20	1.66	1.6×10^{-2}
	GO:0000502	Proteasome complex	7 of 61	1.55	4.5×10^{-6}

FDR, false discovery rate; NADH, Nicotinamide Adenine Dinucleotide (NAD) + Hydrogen (H).

Table 2. KEGG pathway analyzed from the STRING database.

Cell type	Pathway	Description	Count in network	Strength	FDR
HCT-EV	hsa00190	Oxidative phosphorylation	6 of 128	1.24	0.00026
	hsa03010	Ribosome	4 of 131	1.05	0.0158
	hsa04714	Thermogenesis	6 of 226	0.99	0.002
HBR-EV	hsa04130	SNARE interactions in vesicular transport	4 of 32	1.64	0.00045
	hsa04141	Protein processing in endoplasmic reticulum	8 of 163	1.23	1.03×10^{-5}
	hsa03010	Ribosome	6 of 131	1.20	0.00045
PMF-EV	hsa04966	Collecting duct acid secretion	3 of 24	1.73	0.0053
	hsa04721	Synaptic vesicle cycle	3 of 72	1.25	0.0398
	hsa03010	Ribosome	5 of 131	1.21	0.0053
	hsa04141	Protein processing in endoplasmic reticulum	5 of 163	1.12	0.0053
PBR-EV	hsa03050	Proteasome	4 of 43	1.46	0.0045

KEGG, Kyoto Encyclopedia of Genes and Genomes.

Table 3. The functional enrichment analysis of the KEGG pathway.

KEGG Pathways			
Pathway ID	Pathway description	Count in gene set	False discovery rate
HCT-EV			
3010	Ribosome	11	2.82×10^{-11}
HBR-EV			
3010	Ribosome	11	1.54×10^{-11}
PMF-EV			
3010	Ribosome	12	2.70×10^{-13}
PBR-EV			
3050	Proteasome	9	1.74×10^{-11}
3020	RNA polymerase	3	0.02

Discussion

BR cells in CRC are considered chemotherapy resistant [16]. However, the mechanism by which BR cells induce resistance to treatment or the tumor microenvironment remains unclear. Many studies revealed that EVs indicate cellular origin and release important molecules such as proteins or nucleic acids, representing the pathology of patients and cancer development [9,13,17,18]. Our proteomic re-

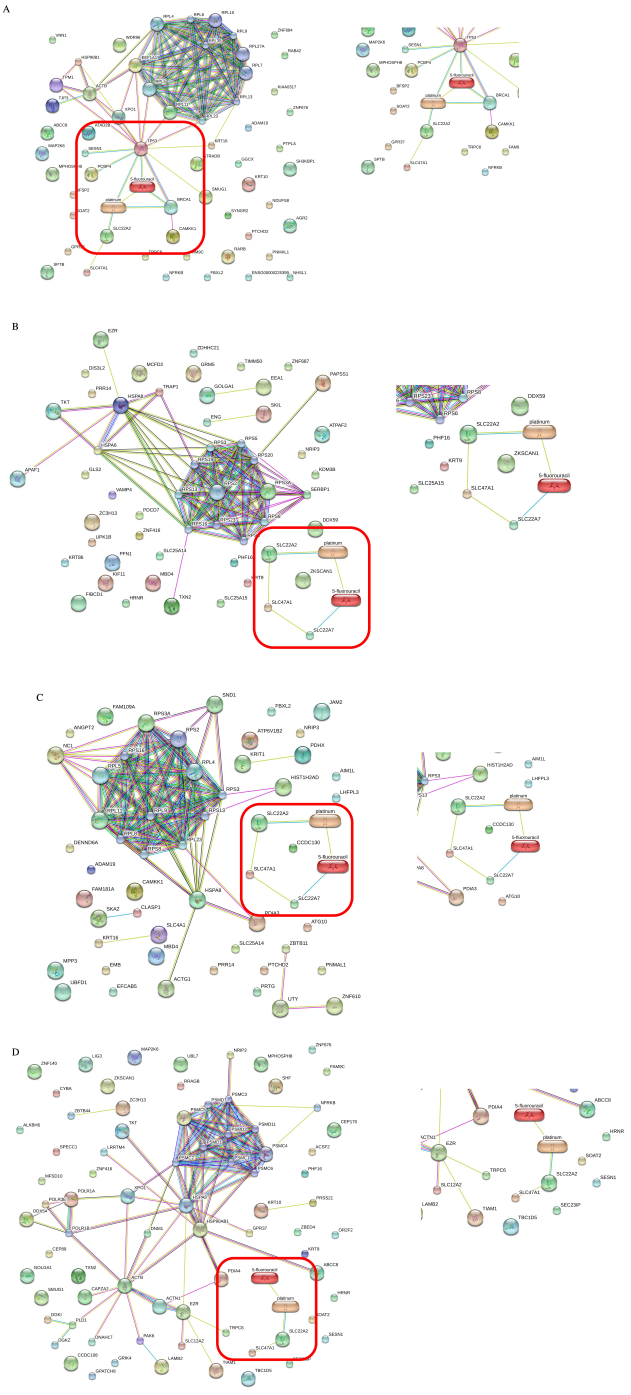

E

Protein-Protein Network Stats	HCT-EV	HBR-EV	PMF-EV	PBR-EV
number of nodes	58	55	54	77
number of edges	90	92	98	103
average node degree	3.1	3.35	3.63	2.68
clustering coefficient	0.922	0.928	0.905	0.862
expected number of edges	46	33	38	52
PPI enrichment p-value	4.46 x 10^{-9}	0.00	6.66 x 10^{-16}	2.40 x 10^{-10}

Fig. 5. Protein-protein and drugs interaction network of a unique protein in each cell type from the STITCH database. The interaction of EVs from HCT (A), HBR (B), PMF (C), and PBR (D) were illustrated. The protein network status of EVs from each group (E). The red box showed protein-drugs correlation. PPI, protein-protein interaction.

Table 4. The top 15 up and downregulated proteins in HBR-EV compared with HCT-EV, identified from the Volcano plot.

	Up		Down	
	Protein	logFC	Protein	logFC
HBR-HCT	PFN1	0.79	G8XUU7	–5.5
	B4DMI9	1.26	E7ET48	–5.14
	LAMB2	1.98	B4DK06	–4.97
	B3KME6	2.19	A8K237	–4.14
	B3KNL3	2.21	Q5VZM0	–3.2
	Q53FZ9	2.35	Q96M20	–2.73
	Q9HB62	2.39	Q69YG3	–2.71
	H3BRI8	2.48	B4DS20	–2.7
	Q5VVC8	2.63	B4E2P8	–2.61
	H0YGA8	2.72	Q96D88	–2.54
	Q86VZ3	3.16	Q59H97	–2.39
	B2RAN2	3.57	G3V277	–2.38
	Q53G91	3.64	E9PP73	–2.38
	O43708	4.47	C9J9N1	–2.11
	Q5VW36	4.66	L0EQU5	–2.07

Table 5. The top 15 up and downregulated proteins in PBR-EV compared with PMF-EV, identified from the Volcano plot.

	Up		Down	
	Protein	logFC	Protein	logFC
PBR-PMF	NPEPPS	1.51	B4DI83	–5.77
	O15354	1.55	Q9HBP3	–4.29
	Q8IVQ6	1.62	Q59EA4	–4.21
	E9PFI5	2.02	H3BRI8	–3.67
	Q5VSN0	2.07	F8VPE9	–3.07
	Q9P225	2.12	Q59ES2	–3.03
	H0YLT7	2.18	E7ET48	–3.02
	F8WD59	2.26	F8WDN2	–2.98
	O75132	2.48	H7C3S5	–2.91
	Q59HA1	2.54	B2R7W6	–2.89
	K9JA46	2.57	K7EIX6	–2.79
	Q53EL8	2.73	F8WEL6	–2.61
	Q8N539	3.11	G3V277	–2.59
	H0Y5I5	3.62	D3DQ69	–2.59
	B4DL56	3.89	I3L3D5	–2.42

sults confirmed that BR cells still represent their PT cells, as indicated by the shared proteins between both cell types (depicted in a Venn diagram).

Several mechanisms are correlated with cancer drug resistance, such as overexpression of drug transport of the ATP-binding cassette, direct export of cytotoxic drugs, or conferring resistance to drug-sensitive cells [19]. EVs contribute to cancer cell metastasis, including promoting cell migration and invasion, establishing a premetastatic niche, and remodeling the extracellular matrix [8,20]. In our findings, proteins correlated with cell proliferation (proline-

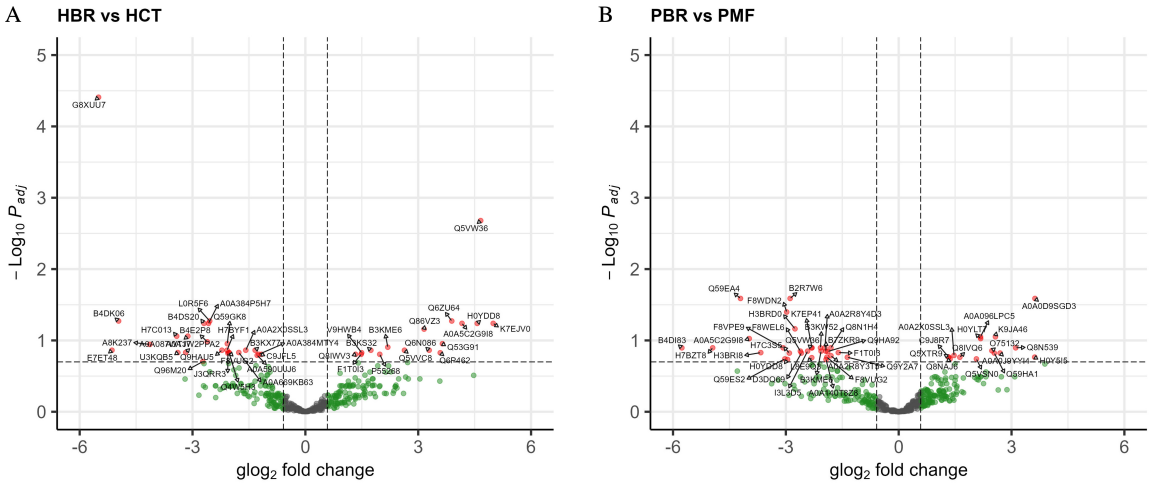

Fig. 6. Volcano plot of the significantly up-regulated (upper-right quadrant) and down-regulated (upper-left quadrant) proteins. Volcano plot of HBR-EVs compared to HCT-EV (A) and PBR-EV compared to PMF-EV (B).

rich protein 14 (PRR14) and NPEPPS), cell cycle control (HSP90AA1), and carcinogenesis (DLGAP5) were up-regulated in EVs from BR cells. This may be due to cell-to-cell communication, which results in tumor progression. Overexpression of (PRR14) has been reported to be a marker of colon cancer progression and metastasis [21]. Data from protein-protein interactions showing proteasome-related proteins were found in the analysis of BR-derived EVs. This may be correlated with reduced drug effectiveness. We also identified proteasome-related proteins (DLGAP5 and NPEPPS) in both HBR- and PBR-derived EVs. Previous data indicated Oxa and 5-FU resistance in HBR and PBR cells. Proteasomal proteins in EVs derived from BR cells may confer their resistant phenotype upon normal cells. NPEPPS overexpression increases cisplatin resistance by preventing cisplatin uptake by bladder tumors [22,23]. The correlation between high expression of disc large associated protein family (DLGAP5) and gallbladder cancer proliferation, migration, and poor prognosis has been previously elucidated [24]. These molecules are encapsulated in EVs and released by the cells, which results in their transport and induction in the tumor microenvironment, leading to tumor growth and the development of resistance to anti-cancer drugs.

Meanwhile, proteins involved in anti-apoptotic function (TXN2), shear stress-activated response (WARS), and tumor suppression (TP53) were found to have reduced, leading to an accumulation of these molecules in cells and resulting in an anti-apoptotic response that could be involved in the resistance to anti-tumor agents. Tryptophanyl-tRNA synthetase (WARS) is highly expressed and is a potential prognostic marker of metastasis in oral, ovarian, pancreatic, and colorectal cancers [25,26].

However, the results of protein-drug interactions only show a correlation between drugs and their related proteins. These correlations require further elucidation. The effects of EVs on cancer cells also require clarification to understand of resistance mechanisms and treatment management better.

Conclusions

Our proteomic analysis of EVs from BR CRC cells expands our understanding of drug resistance mechanisms. These cells release proteins during cell proliferation and cell cycle control, enhancing carcinogenesis. Furthermore, we identified a protein with reduced antitumor drug uptake, underscoring the complexity of drug resistance. Delving deeper into the mechanisms underlying drug resistance can pave the way for more effective strategies to overcome drug resistance in clinical practice.

Availability of Data and Materials

The data that support the findings of this study are available from the corresponding author (Raphatphorn Navakanitworakul), upon reasonable request (nraphatp@medicine.psu.ac.th).

Author Contributions

RN, SS, and SR conceptualized and designed the study; KN developed the methodology; SR, SS and KL provided the software, the formal analysis, data curation; KN conducted the formal analysis, investigation, data curation, draft preparation; RN was involved in reviewing and editing the manuscript and supervised the research. All authors contributed significantly to editorial changes of important content. All authors have read and agreed to the published version of the manuscript. All authors have sufficiently participated in the work to assume public responsibility for appropriate portions of the content and have agreed to be accountable for all aspects of the work, ensuring the accuracy and integrity of the manuscript.

Ethics Approval and Consent to Participate

This project is exempt from the Research Ethics Committee (REC) Faculty of Medicine, Prince of Songkla University's review process under reference number REC6337942.

Acknowledgment

The authors would like to thank Editage (https://www.editage.com) for the English language review.

Funding

This research was supported by the Faculty of Medicine, Prince of Songkla University [Grant number REC6337942]; and the Postdoctoral Fellowship Program, Prince of Songkla University.

Conflict of Interest

The authors declare no conflict of interest.

Supplementary Material

Supplementary material associated with this article can be found, in the online version, at https://doi.org/10.24976/Discov.Med.202436185.121.

References

[1] Karthika C, Sureshkumar R, Zehravi M, Akter R, Ali F, Ramproshad S, *et al*. Multidrug Resistance in Cancer Cells: Focus on a Possible Strategy Plan to Address Colon Carcinoma Cells. Life. 2022; 12: 811.

[2] Wang M, Liu X, Chen T, Cheng X, Xiao H, Meng X, *et al*. Inhibition and potential treatment of colorectal cancer by natural compounds *via* various signaling pathways. Frontiers in Oncology. 2022; 12: 956793.

[3] Louis P, Flint HJ. Diversity, metabolism and microbial ecology of butyrate-producing bacteria from the human large intestine. FEMS Microbiology Letters. 2009; 294: 1–8.

[4] Kang HR, Choi HG, Jeon CK, Lim SJ, Kim SH. Butyrate-mediated acquisition of chemoresistance by human colon cancer cells. Oncology Reports. 2016; 36: 1119–1126.

[5] Nittayaboon K, Leetanaporn K, Sangkhathat S, Roytrakul S, Navakanitworakul R. Cytotoxic effect of metformin on butyrate-resistant PMF-K014 colorectal cancer spheroid cells. Biomedicine & Pharmacotherapy. 2022; 151: 113214.

[6] Nittayaboon K, Leetanaporn K, Sangkhathat S, Roytrakul S, Navakanitworakul R. Characterization of Butyrate-Resistant Colorectal Cancer Cell Lines and the Cytotoxicity of Anticancer Drugs against These Cells. BioMed Research International. 2022; 2022: 6565300.

[7] Yang Q, Xu J, Gu J, Shi H, Zhang J, Zhang J, *et al*. Extracellular Vesicles in Cancer Drug Resistance: Roles, Mechanisms, and Implications. Advanced Science. 2022; 9: e2201609.

[8] Qiao F, Pan P, Yan J, Sun J, Zong Y, Wu Z, *et al*. Role of tumor derived extracellular vesicles in cancer progression and their clinical applications (Review). International Journal of Oncology. 2019; 54: 1525–1533.

[9] Zhao Z, Fan J, Hsu YMS, Lyon CJ, Ning B, Hu TY. Extracellular vesicles as cancer liquid biopsies: from discovery, validation, to clinical application. Lab on a Chip. 2019; 19: 1114–1140.

[10] Pathan M, Keerthikumar S, Ang CS, Gangoda L, Quek CYJ, Williamson NA, *et al*. FunRich: An open access standalone functional enrichment and interaction network analysis tool. Proteomics. 2015; 15: 2597–2601.

[11] Thomas PD, Campbell MJ, Kejariwal A, Mi H, Karlak B, Daverman R, *et al*. PANTHER: a library of protein families and subfamilies indexed by function. Genome Research. 2003; 13: 2129–2141.

[12] Keerthikumar S, Chisanga D, Ariyaratne D, Al Saffar H, Anand S, Zhao K, *et al*. ExoCarta: A Web-Based Compendium of Exosomal Cargo. Journal of Molecular Biology. 2016; 428: 688–692.

[13] Monnamorn L, Seree-Aphinan C, Molika P, Vichitkunakorn P, Pattanapanyasat K, Khwannimit B, *et al*. The Concentration of Large Extracellular Vesicles Differentiates Early Septic Shock From Infection. Frontiers in Medicine. 2021; 8: 724371.

[14] Molika P, Bissanum R, Surachat K, Pattanapanyasat K, Hanprasertpong J, Chotigeat W, *et al*. Exploration of Extracellular Vesicle Long Non-Coding RNAs in Serum of Patients with Cervical Cancer. Oncology. 2024; 102: 53–66.

[15] Abdel-Fatah TMA, Albarakati N, Bowell L, Agarwal D, Moseley P, Hawkes C, *et al*. Single-strand selective monofunctional uracil-DNA glycosylase (SMUG1) deficiency is linked to aggressive breast cancer and predicts response to adjuvant therapy. Breast Cancer Research and Treatment. 2013; 142: 515–527.

[16] Saus E, Iraola-Guzmán S, Willis JR, Brunet-Vega A, Gabaldón T. Microbiome and colorectal cancer: Roles in carcinogenesis and clinical potential. Molecular Aspects of Medicine. 2019; 69: 93–106.

[17] Sadovska L, Eglītis J, Linē A. Extracellular Vesicles as Biomarkers and Therapeutic Targets in Breast Cancer. Anticancer Research. 2015; 35: 6379–6390.

[18] Heck KA, Lindholm HT, Niederdorfer B, Tsirvouli E, Kuiper M, Flobak Å, *et al*. Characterisation of Colorectal Cancer Cell Lines through Proteomic Profiling of Their Extracellular Vesicles. Proteomes. 2023; 11: 3.

[19] Maacha S, Bhat AA, Jimenez L, Raza A, Haris M, Uddin S, *et al*. Extracellular vesicles-mediated intercellular communication: roles in the tumor microenvironment and anti-cancer drug resistance. Molecular Cancer. 2019; 18: 55.

[20] Han L, Lam EWF, Sun Y. Extracellular vesicles in the tumor microenvironment: old stories, but new tales. Molecular Cancer. 2019; 18: 59.

[21] Li F, Zhang C, Fu L. PRR14 overexpression promotes cell growth, epithelial to mesenchymal transition and metastasis of colon cancer via the AKT pathway. PLoS ONE. 2019; 14: e0218839.

[22] Jones RT, Goodspeed A, Akbarzadeh MC, Scholtes M, Vekony H, Jean A, *et al*. The M1 aminopeptidase NPEPPS is a novel regulator of cisplatin sensitivity. bioRxiv. 2021. (preprint)

[23] Scholtes MP, Akbarzadeh M, Romal S, van Dijk M, Kan TW, Mahmoudi T, *et al*. Targeting NPEPPS overcomes cisplatin resistance in patient-derived bladder cancer tumoroids. Cancer Research. 2023; 83: 2852.

[24] Tang X, Zhou H, Liu Y. High Expression of DLGAP5 Indicates Poor Prognosis and Immunotherapy in Lung Adenocarcinoma and Promotes Proliferation through Regulation of the Cell Cycle. Disease Markers. 2023; 2023: 9292536.

[25] Zhou Z, Sun B, Nie A, Yu D, Bian M. Roles of Aminoacyl-tRNA Synthetases in Cancer. Frontiers in Cell and Developmental Biology. 2020; 8: 599765.

[26] Lu S, Wang LJ, Lombardo K, Kwak Y, Kim WH, Resnick MB. Expression of Indoleamine 2, 3-dioxygenase 1 (IDO1) and Tryptophanyl-tRNA Synthetase (WARS) in Gastric Cancer Molecular Subtypes. Applied Immunohistochemistry & Molecular Morphology. 2020; 28: 360–368.